Effect of Wall Shear Stress Gradient on Cells:
Distribution of Deformation and Rotation

Hiroki YONEZAWA

Biomedical Engineering, Systems Design, Kogakuin University
Tokyo, 163-8677, Japan

Shigehiro HASHIMOTO

Biomedical Engineering, Department of Mechanical Engineering, Kogakuin University
shashimoto@cc.kogakuin.ac.jp   Tokyo, 163-8677, Japan

Ryuya ONO

Biomedical Engineering, Department of Mechanical Engineering, Kogakuin University
Tokyo, 163-8677, Japan

ABSTRACT[1]

The effect of wall shear stress gradient on the deformation and rotation of each cell was investigated *in vitro*. To make a Couette-type of shear flow, the culture medium fluid was sandwiched with a constant gap between parallel walls: a lower stationary culture disk, and an upper rotating disk. Mouse fat precursor cells (3T3-L1) were used in this experiment. After cultivation without flow for 24 hours for adhesion of cells on the lower plate, a shear stress of less than 2 Pa was continuously applied to cells for 24 hours in the incubator. The behavior (deformation and major axis angle) of each single cell was tracked using time-lapse images observed by an inverted phase contrast microscope placed in the incubator. For wall shear stresses of less than 1.9 Pa, each cell exhibited active behavior: migration, deformation, and rotation. Whereas, the cells transformed into spheres when wall shear stress was higher than 1.9 Pa. In addition, the cells were observed to tilt against for a wall shear stress gradient approaching 50 Pa/m.

Keywords: Biomedical Engineering, Shear Stress Field, Deformation and 3T3-L1 cells.

1. INTRODUCTION

The effect of shear stress gradients on the endothelial cells of blood vessels exposed to different blood flow conditions is an important predictor of vascular disease, and this topic has been investigated by many research groups [1-7]. In a previous study by our group using the vortex flow generated by the swinging plate *in vitro*, C2C12 cells changed their orientation from parallel to perpendicular with the direction of the flow, although HUVEC made orientation parallel to the direction of the flow [8].

This result is consistent with the behavior of endothelial cells to an increase in wall shear stress: elongation [2], tilting to the streamline [3], migration [4], deformation [5], division [6], and exfoliation [7] from the wall of the scaffold. In the Poiseuille type of flow, the shear rate depends on the distance from the wall: highest at the wall. In the Couette type of flow, on the other hand, the shear rate is constant regardless of the distance from the wall.

A biological cell shows various actions on the scaffold: migration, deformation, rotation, and division. In several cases, cells are exposed to the shear stress both in vivo and in vitro. The direction of the shear stress field also affects the response of each cell [9].

In the present *in vitro* study, an experimental system exhibiting Couette-type flow in the gap between rotating disks was designed to apply a shear stress to cells during incubation, and while under the microscopic observation. The effect of the wall shear stress gradient (1-50 Pa/m) on a single cell (deformation and rotation) was studied.

2. METHODS

Shear Stress Field
To apply the constant shear stress field to the cell culture, a Couette-type of shear flow device has been used (Fig. 1). The shear field is generated between a rotating disk and a stationary dish. The medium fluid is sheared between a rotating wall and a stationary wall. The stationary wall is the scaffold surface of the bottom of the culture dish (diameter 60 mm). In the device, the shear rate (γ) in the medium fluid is calculated by Eq. (1).

$$\gamma = r\,\omega\,/\,d \qquad (1)$$

In Eq. (1), ω is the angular velocity [rad/s], and d is the gap [m] between the wall of the moving disk and the wall of the stationary plate. Between the parallel walls, d is constant. The shear rate (γ [s^{-1}]) in the gap between walls increases in proportion to the distance (r [m]) from the axis of the rotation.
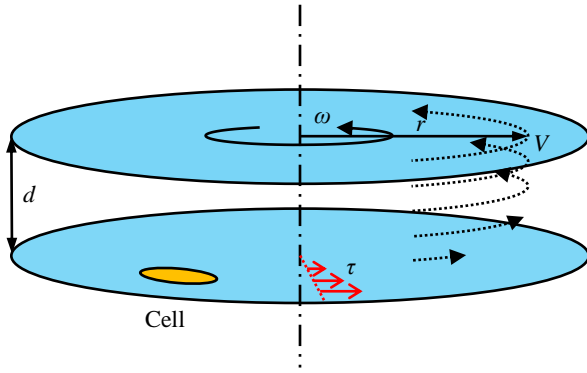

Fig. 1: Couette flow (velocity (V) distribution) between rotating (angular velocity ω) wall and stationary wall at r (radius): distance between walls (d): wall shear stress (τ).

Couette type flow in the tangential direction is formed with a medium filled between the wall of the moving disk and the wall of the stationary plate. Along the d direction, the shear rate (γ) is the same as the wall shear rate. At the circumferential position of the same r, the shear rate (γ) is constant in the gap between the wall of the moving disk and the wall of the stationary plate. The wall shear rate gradient (G) [s^{-1} m^{-1}] is formed in the direction of r.

$$G = \gamma\,/\,r = \omega\,/\,d \qquad (2)$$

The wall shear rate gradient is independent of r. The wall shear rate gradient is constant along r. The angular velocity (11 rad/s < ω < 44 rad/s) was controlled by the stepping motor. In the observation area of the microscope, r varies between 17 mm and 18 mm. The distance d, which was measured by the positions of the focus of the walls at the microscope, was around 0.6 mm. The shear rates (3.3×10^2 s^{-1} < γ < 13×10^2 s^{-1}) are made in the present experiment by adjustment of these parameters.

The wall shear stress (τ [Pa]) is calculated using the viscosity (η [Pa s]) of the medium.

$$\tau = \eta\,\gamma \qquad (3)$$

Using the viscosity of the medium of 1.5×10^{-3} Pa s (measured by a cone and plate viscometer at 310 K), the wall shear stress τ has been calculated (0.45 Pa < τ < 2

Pa). The wall shear stress gradient (τ_g [Pa/m]) on the scaffold plane is calculated by Eq. (4).

$$\tau_g = \tau\,/\,r = \eta\,\gamma\,/\,r = \eta\,G = \eta\,\omega\,/\,d \qquad (4)$$

The wall shear stress gradient is independent of r. The wall shear stress gradient is constant along r.

The rotating disk device was mounted on the stage of the inverted phase contrast microscope placed in the incubator. The device allows the microscopic observation of cells cultured on the stationary wall during exposure to the shear flow field.

Cell
3T3-L1 (mouse fat precursor cells, a cell line derived from cells of mouse 3T3) was used in the test. Cells were cultured in D-MEM (Dulbecco's Modified Eagle's Medium): containing 10% decomplemented FBS (fetal bovine serum), and 1% penicillin/ streptomycin.

The cells were seeded on the dish at the density of 3000 cells/cm^2. To make adhesion of cells to the bottom of the culture dish, the cells were cultured for 24 hours in the incubator without flow stimulation (without rotation of the disk). After the pre-incubation for 24 hours without shear, the cells were continuously sheared with the rotating disk for 24 hours in the incubator at the constant rotating speed. The constant speed was preset for each test to keep the designed value of the shear stress.

Time-lapse Images
The time-lapse microscopic images were taken every 5 minutes during the cultivation. To distinguish between cells and background, each image was binarized by setting a threshold. Using the image, the contour of each cell adhered on the stationary plate of the scaffold was traced. Cells with the two-dimensional projected area greater than 100 µm^2 were counted in the following data. The contour of each cell was approximated to ellipse (Fig. 2).
On the ellipse, the length of the major axis (a), and the length of the minor axis (b) were measured. The ratio of axes is calculated as the shape index (P) given by Eq. (5).

$$P = 1 - b\,/\,a \qquad (5)$$

For a circle, $P = 0$. As the ellipse is elongated, P approaches to 1. The counterclockwise angle (θ) of the main axis from the flow direction was measured (Fig. 2).
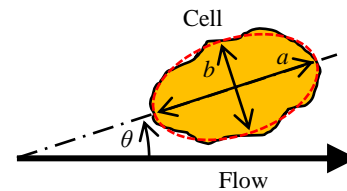

Fig. 2: Shape index and angle of cell exposed to shear flow field.

3. RESULTS

Under the shear flow for 24 hours, cells actively exhibited rotation and deformation, including division. Several cells were exfoliated at the wall shear stress of 2 Pa. Figs. 3-5 show cumulated data in 24 hours: n_0 shows the initial number of cells. In Figs. 3-5, each point corresponds to the data for each cell on each slide of the time-lapse images. Fig. 3 shows the angle (θ) of major axis of each cell related to the shear stress (τ). Fig. 4 shows the shape index (P) of each cell related to the shear stress (τ). Fig. 5 shows the relationships between the shape index (P) and the angle (θ) of major axis of each cell. Figs. 3a, 4a, and 5a show data in the shear stress (τ) range between 0.46 Pa and 0.5 Pa. Figs. 3b, 4b, and 5b show data in the shear stress (τ) range between 0.91 Pa and 1 Pa. Figs. 3c, 4c, and 5c show data in the shear stress (τ) range between 1.18 Pa and 1.26 Pa. Figs. 3d, 4d, and 5d show data in the shear stress (τ) range between 1.82 Pa and 2 Pa. Cells tend to migrate and concentrate to the areas of the shear stress at 0.5 Pa (Figs. 3a and 4a) and 1.9 Pa (Figs. 3d and 4d).

The angle decreases with the increase of the wall shear stress from 0.45 Pa to 0.5 Pa (Fig. 3a). The angle of each cell is distributed not only at 0 degrees but also at ±90 degrees. The angles indicate parallel and perpendicular to the flow, respectively. The angle tends to be negative at the wall shear stress higher than 0.91 Pa (Fig. 3b). Data points widely spread over various angle at the wall shear stress higher than 1.8 Pa (Fig. 3d).

The shape indexes (P) of many cells are higher than 0.5 at the wall shear stress higher than 0.5 Pa (Fig. 4). The shape index (P) is distributed around 0.8 and 0.2, indicating active repetitive deformation of each cell (Fig. 4b). The shape indexes (P) of many cells are lower than 0.5 at the wall shear stress higher than 1.95 Pa (Fig. 4d). As the cell shape approaches the sphere, the shape index (P) approaches zero. After transforming into a sphere, several cells detached.

Many cells tilt with negative angle with higher shape index (Fig. 5). Several cells tilt with positive angle at the wall shear stress gradient higher than 1.1×10^2 Pa/m (Fig. 5d).
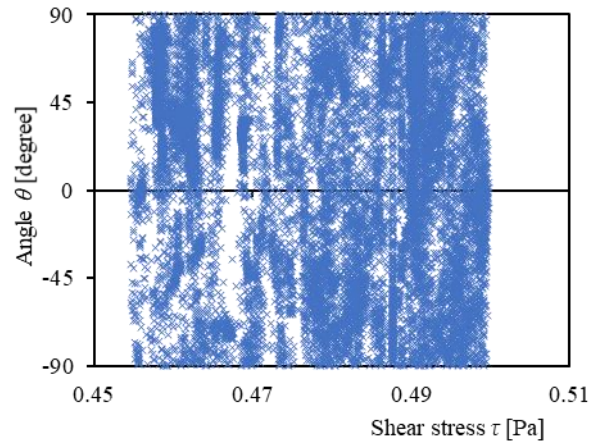

Fig. 3a: Angle θ vs. shear stress (0.46 Pa < τ < 0.5 Pa); 3T3-L1; Initial number of cells n_0 = 47; wall shear stress gradient G = 28 Pa/m.
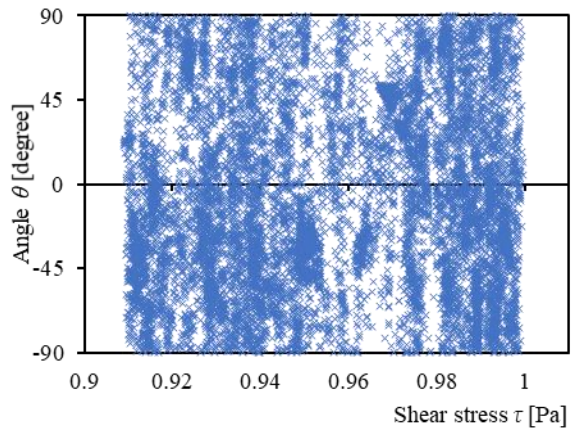

Fig. 3b: Angle θ vs. shear stress (0.91 Pa < τ < 1 Pa); 3T3-L1; n_0 = 37; wall shear stress gradient G = 56 Pa/m.

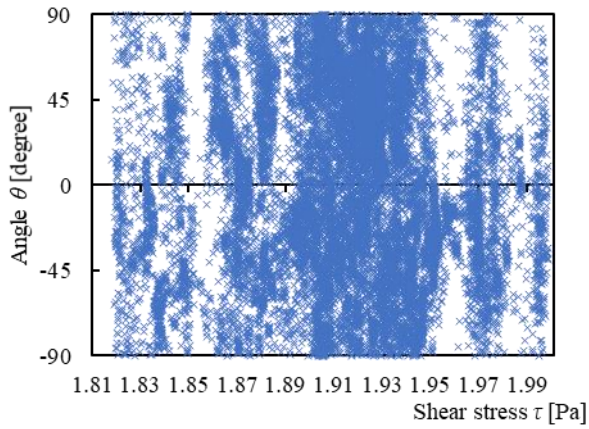**Fig. 3c:** Angle θ vs. shear stress (1.18 Pa < τ < 1.26 Pa); 3T3-L1; n_0 = 46; wall shear stress gradient G = 70 Pa/m.

Fig. 3d: Angle θ vs. shear stress (1.82 Pa $< \tau <$ 2 Pa); 3T3-L1; n_0 = 46; wall shear stress gradient G = 1.1×10^2 Pa/m.

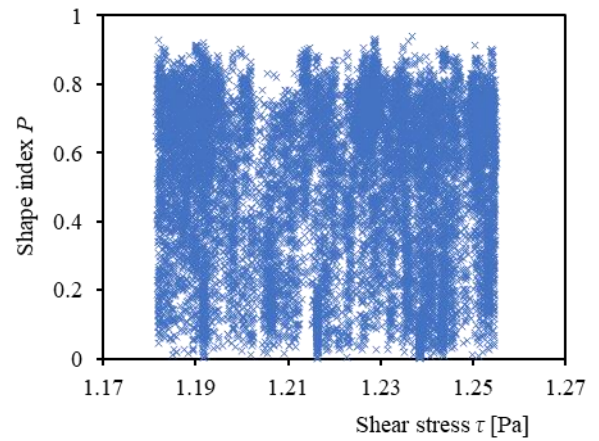**Fig. 4c:** Shape Index P vs. shear stress (1.18 Pa $< \tau <$ 1.26 Pa); n_0 = 46; 3T3-L1; wall shear stress gradient G = 70 Pa/m.

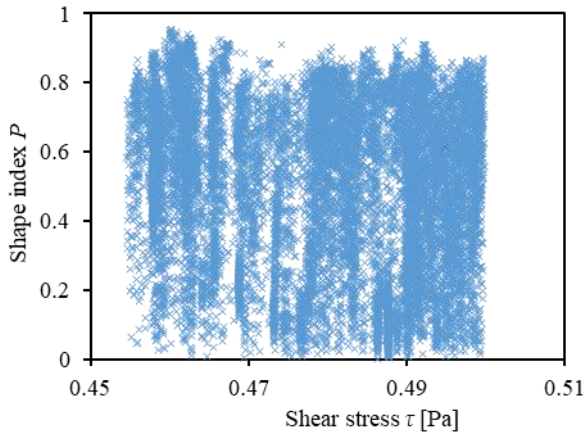**Fig. 4a:** Shape Index P vs. shear stress (0.46 Pa $< \tau <$ 0.5 Pa); 3T3-L1; n_0 = 47; wall shear stress gradient G = 28 Pa/m.
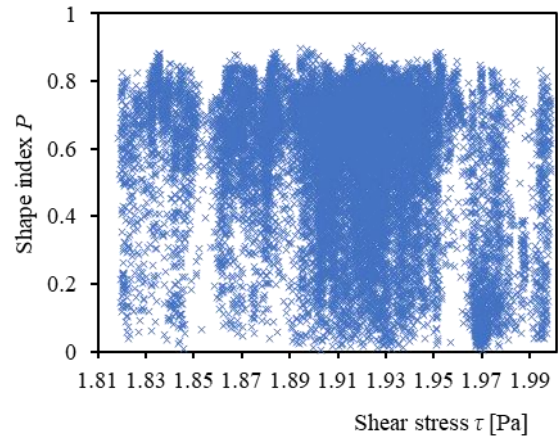

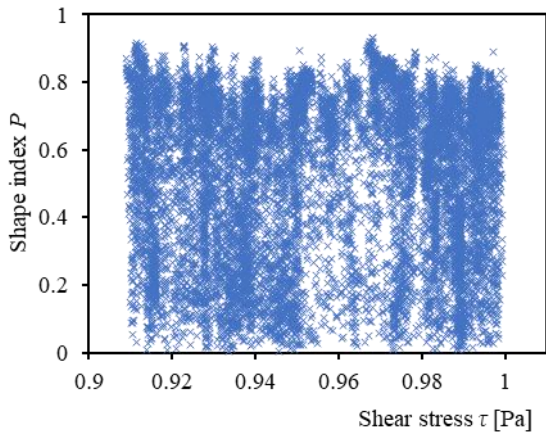**Fig. 4d:** Shape Index P vs. shear stress (1.82 Pa $< \tau <$ 2 Pa); 3T3-L1; n_0 = 46; wall shear stress gradient G = 1.1×10^2 Pa/m.

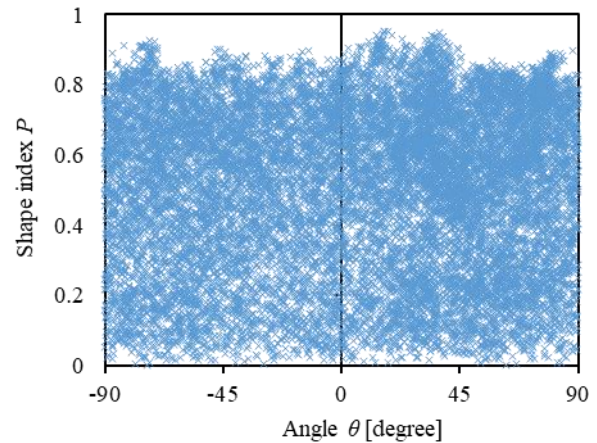**Fig. 4b:** Shape Index P vs. shear stress (0.91 Pa $< \tau <$ 1 Pa); 3T3-L1; n_0 = 37; wall shear stress gradient G = 56 Pa/m.

Fig. 5a: Shape Index P vs. angle; shear stress (0.46 Pa $< \tau <$ 0.5 Pa); 3T3-L1; n_0 = 47; wall shear stress gradient G = 28 Pa/m.

Fig. 5b: Shape Index P vs. angle; shear stress (0.46 Pa < τ < 0.5 Pa); 3T3-L1; n_0 = 37; wall shear stress gradient G = 56 Pa/m.

Fig. 5c: Shape Index P vs. angle; shear stress (1.18 Pa < τ < 1.26 Pa); 3T3-L1; n_0 = 46; wall shear stress gradient G = 70 Pa/m.

Fig. 5d: Shape Index P vs. angle; shear stress (1.82 Pa < τ < 2 Pa); 3T3-L1; n_0 = 46; wall shear stress gradient G = 1.1×10^2 Pa/m.

4. DISCUSSION

A biological cell shows passive and active responses to its environment. When shear stress deforms the profile of a cell, the cell adapts by changing its shape and orientation. While strong stimulation above a threshold damages the cell, stimulation below the threshold remains in the cell as a memory for the response in the next step. The hysteresis effect governs the active response of the cell [9]. In a previous study, cells were exposed to the shear flow in a donut-shaped open channel, and the effect of flow stimulation on cultured cells has been studied *in vitro* [8]. When the flow has an open surface [10], it is difficult to estimate the shear stress value in the fluid. Between two parallel walls, on the other hand, the velocity profile is estimated to be parabolic in the laminar flow.

The Couette-type of flow is convenient to estimate the shear stress in the flow with the constant shear rate between the moving wall and the stationary wall, which is also available to non-Newtonian fluid like a physiological fluid. Several kinds of the devices including Couette-type flow were designed for quantitative experiments of biological fluid in the previous studies [11-15]. The cone-and-plate type device has the uniform shear field in the entire space between the rotating cone and the stationary plate [11]. The shear stress is constant and independent of the distance from the rotating axis. The erythrocyte destruction was studied between the rotating concave cone and the stationary convex cone.

A parallel disk system using a rotating disk and a stationary disk [12], on the other hand, has several advantages: stability of the rotating motion of the disk, stability of the optical path for the microscopic observation, morphologic preciseness of the plane of the disks, and simultaneous observation over the range of variation of the shear rate proportional to the radius from the rotational axis (Eq. (1)). The floating erythrocyte deformation was observed between counter rotating parallel disks [13]. The steady actual flow direction adjacent to the scaffold surface of cell culture has been confirmed by the streamline traced by the direction of exfoliation of the cell and of the moving particle adjacent to the surface [14]. The flow velocity, which increases in proportional to the distance from the rotating axis, has also been confirmed by tracings of the moving particle adjacent to the surface.

The wall shear stress of 1 Pa is typical value on the inner surface of the human blood vessels *in vivo*. Myoblasts tend to migrate to the oblique direction of the lower shear stress field at 1 Pa. The effect of shear flow on cells depends on the cell types [12]. The dependency might be applied to the cell sorting technology. Tracings of the cell after division is convenient to study on the initial behavior of the cell [15]. The cells proliferate
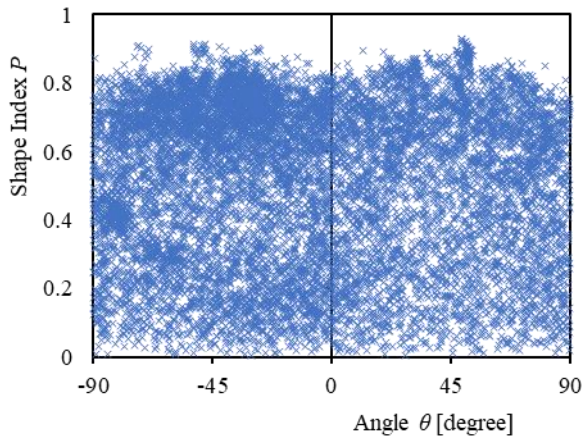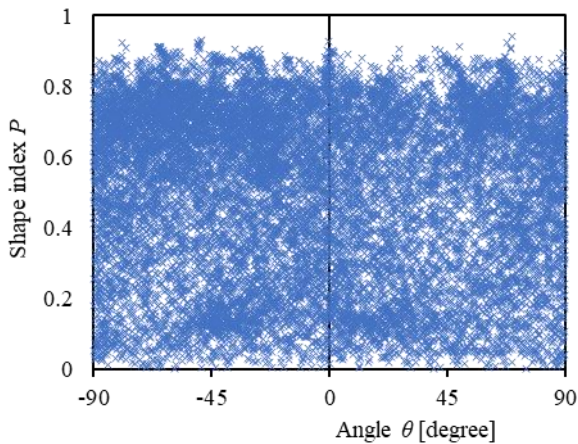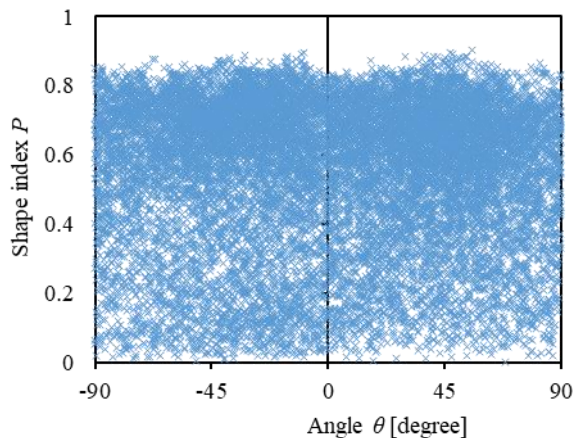
regardless of the shear flow stimulation. The cell cycle did not vary under the shear flow. The deformation of each cell can be tracked by the time-lapse images with the interval of five minutes in the present experiment.

The effect of shear flow on cells was investigated in many previous studies. The shear flow affects adhesion of each cell [16]. Adhesion of cells can be controlled with design of the scaffold [17]. The behavior of cells in the shear flow was simulated in the previous study [18]. The effect of "fluid induced shear stresses" on osteoblasts was measured in a previous study [19].

The effect of shear stress gradient on cells were investigated in the previous study [2, 6]. The wall shear stress gradient can cause the elongated cell (Fig. 6) to rotate counterclockwise. Results of the present experiment shows that the angle (θ) of the major axis of each cell tends to be negative at the wall shear stress gradient around 50 Pa/m (Figs. 3a, 3b and 3c). The moderate wall shear stress gradient promotes active rotation of each cell. The behavior might be active adaptation of each cell. Many cells, on the other hand, have zero degree or positive value of the angle (θ) at the wall shear stress gradient around 100 Pa/m (Figs. 3a, 3b and 3c). The behavior might be passive reaction under the wall shear stress gradient.
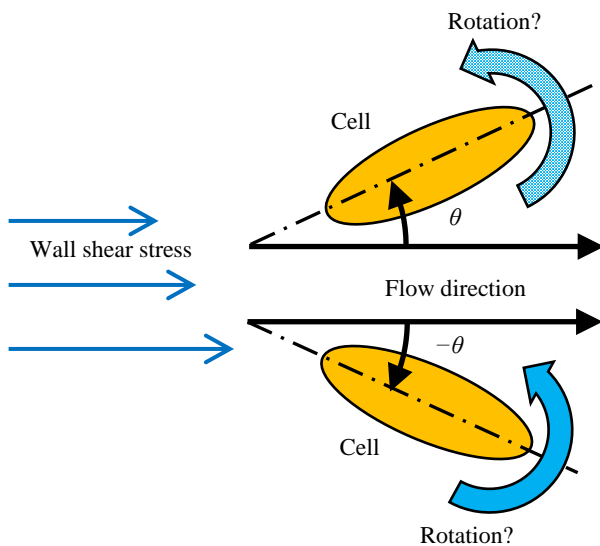

Fig. 6: Angle of cell at wall shear stress gradient; passive counterclockwise rotation of cell due to wall shear stress gradient.

At the time of division, each cell transforms into a sphere. A sphere is a circle on a two-dimensional projection plane. The shape index (P) of the circle is zero. Many cells have a shape index of zero when divided. When

cells are highly active, the data for each cell is widely distributed (Figs. 3b and 4b). Data of the shape index (P) are widely distributed under appropriate values of wall shear stress stimulation (0.5 Pa $< \tau <$ 1 Pa). A moderate wall shear stress promotes active deformation of each cell. Excessive wall shear stress induces detachment of a cell from the culture surface scaffold (Fig. 4d).

Since the initial number of cells within the image corresponding to each figure was not controlled to a constant value, the absolute number of cells cannot be compared beyond the figure number: Figs. 3, 4, and 5. The relative distribution of the data in each figure can be compared, because data in each figure is collected from the same time-lapse image in the same observation area of the experiment.

5. CONCLUSIONS

Both the deformation and orientation of each single cell of 3T3-L1 (mouse fat precursor cells) under a shear stress field around 1 Pa were tracked by time lapse images using a Couette type flow device placed on the stage of the microscope in the incubator. Under wall shear stresses below 1.9 Pa, each cell exhibited active behavior: migration, deformation, and rotation. We found that cells transformed into spheres at the wall for shear stress higher than 1.95 Pa. Many cells tilt against a wall shear when the stress gradient is around 50 Pa/m.

REFERENCES

[1] M. Inglebert, L. Locatelli, D. Tsvirkun, P. Sinha, J.A. Maier, C. Misbah and L. Bureau, "The Effect of Shear Stress Reduction on Endothelial Cells: A Microfluidic Study of the Actin Cytoskeleton", **Biomicrofluidics**, Vol. 14, No. 024115, 2020, pp. 1–14. doi:10.1063/1.5143391

[2] N. DePaola, M.A. Gimbrone Jr., P.F. Davies and C.F. Dewey Jr., "Vascular Endothelium Responds to Fluid Shear Stress Gradients", **Arteriosclerosis Thrombosis and Vascular Biology**, Vol. 12, No. 11, 1992, pp. 1254−1257.

[3] D. Meza, B. Musmacker, E. Steadman, T. Stransky, D.A. Rubenstein, and W. Yin, "Endothelial Cell Biomechanical Responses are Dependent on Both Fluid Shear Stress and Tensile Strain", **Cellular and Molecular Bioengineering**, Vol. 12, No. 4, 2019, pp. 311–325.

[4] M.A. Ostrowski, N.F. Huang, T.W. Walker, T. Verwijlen, C. Poplawski, A.S. Khoo, J.P. Cooke, G.G.

Fuller and A.R. Dunn, "Microvascular Endothelial Cells Migrate Upstream and Align Against the Shear Stress Field Created by Impinging Flow", **Biophysical Journal**, Vol. 106, No. 2, 2014, pp. 366–374.

[5] R. Steward Jr, D. Tambe, C.C. Hardin, R. Krishnan and J.J. Fredberg, "Fluid Shear, Intercellular Stress, and Endothelial Cell Alignment", **American Journal of Physiology–Cell Physiology**, Vol. 308, 2015, pp. C657–C664.

[6] Y. Tardy, N. Resnick, T. Nagel, M.A. Gimbrone Jr and C.F. Dewey Jr, "Shear Stress Gradients Remodel Endothelial Monolayers in Vitro via a Cell Proliferation-Migration-Loss Cycle", **Arteriosclerosis Thrombosis and Vascular Biology**, Vol. 17, No. 11, 1997, pp. 3102–3106.

[7] P. Feugier, R.A. Black, J.A. Hunt and T.V. How, "Attachment, Morphology and Adherence of Human Endothelial Cells to Vascular Prosthesis Materials under the Action of Shear Stress", **Biomaterials**, Vol. 26, 2005, pp. 1457–1466.

[8] S. Hashimoto and M. Okada, "Orientation of Cells Cultured in Vortex Flow with Swinging Plate In Vitro", **Journal of Systemics Cybernetics and Informatics**, Vol. 9, No. 3, 2011, pp. 1−7.

[9] S. Hashimoto, Y. Morita, H. Yonezawa and Y. Endo, "Behavior of Cell on Micro Ridge Pattern after Continuous Stimulation of Tangential Force", **Proc. 12th International Multi-Conference on Complexity Informatics and Cybernetics**, Vol. 2, 2021, pp. 7−12.

[10] P. Limraksasin, Y. Kosaka, M. Zhang, N. Horie, T. Kondo, H. Okawa, M. Yamada and H. Egusa, "Shaking Culture Enhances Chondrogenic Differentiation of Mouse Induced Pluripotent Stem Cell Constructs", **Scientific Reports**, Vol. 10, No. 14996, 2020, pp. 1–15.

[11] S. Hashimoto, H. Sugimoto and H. Hino, "Behavior of Cell in Uniform Shear Flow Field between Rotating Cone and Stationary Plate", **Journal of Systemics Cybernetics and Informatics**, Vol. 16, No. 2, 2018, pp. 1−7.

[12] S. Hashimoto, H. Sugimoto and H. Hino, "Effect of Couette Type of Shear Stress Field with Axial Shear Slope on Deformation and Migration of Cell: Comparison between C2C12 and HUVEC", **Journal of Systemics Cybernetics and Informatics**, Vol. 17, No. 2, 2019, pp. 4-10.

[13] S. Hashimoto, "Detect of Sublethal Damage with Cyclic Deformation of Erythrocyte in Shear Flow", **Journal of Systemics Cybernetics and Informatics**, Vol. 12, No. 3, 2014, pp. 41-46.

[14] S. Hashimoto, H. Sugimoto, H. Hino, "Behavior of Cell in Uniform Shear Flow Field between Rotating Cone and Stationary Plate", **Journal of Systemics Cybernetics and Informatics**, Vol. 16, No. 2, 2018, pp. 1-7.

[15] S. Hashimoto, H. Yonezawa and R. Ono, "Cell Activity Change After Division under Wall Shear Stress Field", **Proc. ASME International Mechanical Engineering Congress & Exposition** (IMECE2021), 2021, pp. 1-8.

[16] Z. Zhang, J. Du, Z. Wei, Z. Chen, C. Shu, Z. Wang and M. Li, "Numerical Investigation of Adhesion Dynamics of a Deformable Cell Pair on an Adhesive Substrate in Shear Flow", **Physical Review E**, Vol. 100, No. 3, 2019.

[17] F.P.W. Melchels, B. Tonnarelli, A.L. Olivares, I. Martin, D. Lacroix, J. Feijen, D.J. Wendt and D.W. Grijpma, "The Influence of the Scaffold Design on the Distribution of Adhering Cells after Perfusion Cell Seeding", **Biomaterials**, Vol. 32, No. 11, 2011, pp. 2878−2884.

[18] P. Bagchi, P.C. Johnson and A.S. Popel, "Computational Fluid Dynamic Simulation of Aggregation of Deformable Cells in a Shear Flow", **Journal of Biomechanical Engineering**, Vol. 127, No. 7, 2005, pp. 1070−1080.

[19] W. Yu, H. Qu, G. Hu, Q. Zhang, K. Song, H. Guan, T. Liu and J. Qin, "A Microfluidic-Based Multi-Shear Device for Investigating the Effects of Low Fluid-Induced Stresses on Osteoblasts", **PLoS ONE**, Vol. 9, No. 2, 2014, pp. 1−7.